Energy and mechanical aspects on the thermal activation of diaphragm walls for heating and cooling

Accepted Manuscript

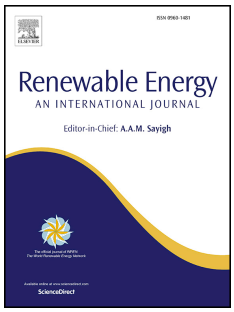

Energy and mechanical aspects on the thermal activation of diaphragm walls for heating and cooling

Marco Barla, Alice Di Donna, Alessandro Santi

PII: S0960-1481(18)31258-8

DOI: https://doi.org/10.1016/j.renene.2018.10.074

Reference: RENE 10724

To appear in: *Renewable Energy*

Received Date: 26 June 2018

Revised Date: 10 October 2018

Accepted Date: 16 October 2018

Please cite this article as: Barla M, Di Donna A, Santi A, Energy and mechanical aspects on the thermal activation of diaphragm walls for heating and cooling, *Renewable Energy* (2018), doi: https://doi.org/10.1016/j.renene.2018.10.074.

Energy and mechanical aspects on the thermal activation of diaphragm walls for heating and cooling

Marco Barla, Alice Di Donna, Alessandro Santi*

Dept. of Structural, Building and Geotechnical Engineering, Politecnico di Torino, Italy

* Corresponding author: marco.barla@polito.it

Abstract

Underground geotechnical structures, such as deep and shallow foundations, diaphragm walls, tunnel linings and anchors are being increasingly employed as energy geostructures to exchange heat with the ground by installing absorber pipes into the structural elements. This paper focuses on the application of this technology to reinforced concrete diaphragm walls used for construction of underground car parks, basements and metro stations, with the purpose of heating and cooling the adjacent buildings. Preliminary numerical modelling allowed optimising the geothermal plant design of the diaphragm wall. Then its energy efficiency is investigated through finite element thermo-hydro coupled analyses together with the effects of the thermal activation on the surrounding soil. Finally, finite difference thermo-mechanical analyses are used to study the mechanical effects induced by the thermal activation.

Keywords: energy walls, energy geostructures, thermo-hydraulic numerical analyses, thermo-mechanical numerical analyses, shallow geothermal energy

1. Introduction

Underground geotechnical structures, such as deep and shallow foundations, diaphragm walls, tunnel linings and anchors are being increasingly employed as energy geostructures, in Europe and all around the world [1,2]. Research studies on this technology are increasingly being carried out, including investigations on their energy efficiency and geotechnical behaviour [3–7]. Besides being constructed for their primary structural role, they are equipped to be able to exchange heat with the ground and supply thermal energy for heating and cooling of buildings and de-icing of infrastructures. This technology can play a fundamental role in the current challenge of facing the increasing need for clean and renewable sources of energy. The thermal activation is achieved by installing absorber pipes in the geostructures, in which a circulating fluid extracts or injects heat from or into the ground. The polyethylene Pe-Xa pipes are usually attached to the reinforcing steel cage, before concrete cast. The pipes inlet/outlet of each panel are connected to the main circuit, which links them to the heat pumps.

These systems belong to the category of low enthalpy geothermal plants and are associated with heat pumps. A number of real applications of this technology are already operational especially in Austria, Germany, United Kingdom and Switzerland [8–15].

This paper focuses mainly on the application of this technology to the diaphragm walls of underground car parks, basements and metro stations, with the purpose of using them for heating and cooling the adjacent buildings. Efforts have already been devoted to study similar applications [4,16–19] and a number of real operational systems exist [20–22].

The main goals of this study were to optimise the heat exchanger pipe circuit in the walls, quantify the extractable and injectable heat, and study the consequences in terms of structural behaviour and effects on the surrounding ground.

A reference diaphragm wall, with the geometry shown in Figure 1 was considered in all the simulations presented in this paper, i.e. a wall panel 2.5 m wide, 0.8 m thick and 15.5 m deep. The absorber pipes are installed only on the ground side. Another solution would have been to have a double circuit, one on each

side, in order to foster the heat exchange with the air inside the excavation. The efficiency of this solution needs to be checked.

Preliminary numerical analyses were conducted to assess the optimal geothermal plant design for the diaphragm wall. Then, three main aspects were investigated with reference to the optimal setting: the energy performance, the temperature variation in the surrounding soil and the mechanical effects induced on the wall by its thermal activation.

2. Energy performance and thermal aspects

With the aim to assess the energy efficiency of thermo-active walls analysing the thermal exchange between the fluid circulating through the pipes, the concrete structure and the surrounding saturated soil, thermo-hydro simulations were performed through the finite element software FEFLOW© [23]. The procedure adopted is consistent to that described in [24] for energy tunnels.

The thermo-hydro problem is governed by the mass conservation equation, the energy conservation equation and the Darcy's velocity law.

The absorber pipes were reproduced through the 1D discrete features elements provided in the software. The use of these elements to simulate pipes in geothermal systems has been validated and showed good agreement when compared to analytical solutions [23]. In this study, the pipes are considered to have a diameter of 25 mm and thickness of 2.3 mm. The material properties used in the simulations are listed in Table 1. Parameters related to the ground are representative of the Torino (Italy) subsoil, according to previous studies where specific pumping tests were executed [25].

2.1. Study on the pipe configuration and fluid velocity

The geometry of the pipe circuit is a compromise between the construction feasibility and the optimised heat exchange.

Simplified models were built in order to identify the most efficient configuration in terms of heat exchange, depending on the position of the pipes and the fluid velocity. The initial temperature was set equal to 14 °C for the whole domain, while the ground water level was set to 5 m below the ground surface. For the sake of simplicity, no ground water flow was considered in these preliminary analyses. The bottom and far field boundaries (left side in Figure 2a) were checked to be far enough not to influence the results. External air temperature was imposed on the top boundary, considering the seasonal fluctuation in the city of Torino (based on data from [26]), representative of a temperate humid European climate, according to Figure 2b. The choice of the wall thermal boundary condition (interior of the tunnel or car park or basement) is one of the most peculiar aspects of energy walls or tunnels modelling, as it represents a major difference with respect to more conventional borehole heat exchangers or energy piles, which are surrounded by soil [3,6,27]. However, for these preliminary analyses which have the purpose to find the most efficient solution and not to provide reliable data of exchanged heat, adiabatic condition was imposed on the right side of the model. For the thermal-hydraulic analysis, the model was firstly run for one year without activation of the geothermal plant to initialise the soil temperature according to the external air variation. The plant was then activated by injecting water into the pipes at a constant inlet temperature of 4°C for one month (Figure 2b), reproducing the heat extraction condition (winter mode). Three pipe configurations were considered, as illustrated in Figure 3. It has to be noticed that the pipes length is different for the three configurations, i.e. it is 55.5 m for case (a), 68.0 m for case (b) and 50.0 m for case (c). For the three configurations, the analyses were repeated for different values of fluid velocity, between 0.1 and 1.0 m/s. The exchanged heat, expressed in Watt was computed as:

$$Q = mc_w|T_{wo} - T_{wi}| \quad (1)$$

where m is the mass flow rate inside the pipes expressed in kg/s, T_{wo} the fluid outlet temperature and T_{wi} the imposed fluid inlet temperature.

The results obtained for the three pipe configurations and imposing a fluid velocity of 0.6 m/s are reported in Table 2. The exchanged heat per linear meter, Q_l is intended per meter of pipe, while that per square meter, Q_s, is intended per wall surface area. Configuration (c) appears to be the most favourable. This result is in agreement with the outcome of a similar study carried out by [19], although other studies highlighted concerns about the practical applicability of such horizontal configuration [20]. Because of the amount of reinforcement usually used in diaphragm walls, placing pipes horizontally might be more difficult and it may affect the way in which the concrete spreads in the trench to more extent than the vertical placement.
Figure 4 shows the influence of the fluid velocity on the exchanged heat for the pipes configuration (c). All considered velocities allow for a turbulent flow to occur into the pipes. Differently from the case of energy tunnels [3], the fluid velocity does not affect the exchanged heat in a significant manner. However, this was also confirmed by other similar studies on energy piles and walls [4,19,28]. Considering these results and the mentioned difference in pipes length, configuration (c) was chosen as the optimised one in the following, assuming a fluid velocity of 0.2 m/s.

2.2. Quantification of heat exchange potential

A more advanced 3D numerical model was built to properly quantify the exchangeable heat. The model reproduces with more details the geometry of the diaphragm wall by including a 1.0 m thick concrete slab which constitutes the base of the excavation, at 9.5 m below the ground surface (Figure 5a). The surrounding ground is also included with the dimensions shown in the same figure. The bottom, left and right boundaries were checked to be far enough not to influence the results. The same external air temperature seasonal variation was adopted and imposed to the top boundary. The assumption on how to model the internal air was previously studied by [27] and the comparison between different boundary conditions showed that modelling the air is equivalent to consider the wall as adiabatic and was adopted in the following. Air was thus modelled through finite elements, having air thermal properties. This assumption is the most conservative in terms of energy efficiency, because the heat exchange between the wall and the air is neglected. Two groundwater flow conditions were considered: (i) no flow and (b) ground water flow velocity of 1.5 m/d. Based on the previous analysis, the inlet fluid velocity was assumed equal to 0.2 m/s.

The time frame in the analysis is 4 years. The first year reproduces the situation before the activation of the geothermal plant, where only the external air temperature is present. This is followed by three years of heating-cooling mode. A double mode usage of the geothermal plant was considered, including three months heating and three months cooling, according to the input presented in Figure 5b. It is to be mentioned that this condition does not fully reproduce the proper behaviour of a real heat pump system where the temperature of the fluid would be the result of the use of the heat pump and, generally, will not remain constant over a season. Although real systems operate within varying and complex energy demand (and hence inlet temperature) patterns, a constant temperature has been used in the following to provide (a) a simpler and controlled conditions comparison of the parameters under consideration and (b) a more generally applicable approach within the wide range of thermal demand scenarios relevant to different building typologies.

The obtained results are illustrated in Figure 6a and 6b, in terms of inlet/outlet temperature and exchanged heat per meter of wall depth, respectively. It can be concluded that the heat exchange is highly affected by the presence of the ground water flow, as confirmed by similar studies [29]. The peak and end of cycle values of exchanged heat in winter and summer conditions for the two-considered ground water flow velocities are presented in Table 3 and Table 4. It has to be noticed that these results are valid for the considered geometry and conditions, i.e. for the upstream side of the structure.

To quantify the effective benefit in using this technology, the obtained results in terms of heat exchange were compared with the average energy demand of a typical apartment building. Data on energy consumption for heating were extracted from the database delivered by the European project Tabula [30], which provides an overall figure of energy demand in Europe for several typical buildings. The apartment block building

typology for a middle climatic zone (Italy) was selected from the database. As the energy demand seems to be highly influenced by the construction period due to the continuum innovation in the refurbishment process, two construction periods were considered, i.e. early 1900 and after 2006. Two different heat supply systems correspond to the two selected periods, both based on a gas central heating system. A non-condensing boiler (atmospheric burner), central distribution and gas-fired instantaneous water heater was considered for the 1900 constructions while a low temperature standard boiler and gas-fired instantaneous water heater with condensing plus thermal solar plant was considered for most recent constructions. Assuming to turn on the geothermal system for 1800 hours per year for heating during winter, the number of energy wall panels needed for heating was computed. Table 5 illustrates the results of this analysis for both the considered groundwater flow conditions. The number of panels needed for apartment buildings are in line with the geometry that an underground car park for the residents' use would likely have. This is particularly true with the today's figures in terms of energy needs, showing that application of energy geostructures is promising if considered from the design stage of new construction.

2.3. Thermal effects on the surrounding soil

In order to evaluate the influence on the ground temperature, Figure 7 shows its evolution 5 m far from the wall contour, at different depths in the case of no flow and of groundwater flow of 1.5 m/d. Up to about 5.5 m depth (point A in Figure 5) the ground temperature is affected by the external air temperature fluctuation (see first year results). The activation of the geothermal system induces a variation of temperature in both points A and B of +/- 1.5 °C with respect to the temperature variation experienced during the first year of simulation.

3. Thermo-mechanical aspects

When the diaphragm wall is used as ground heat exchanger, it is subjected to seasonally cyclic temperature variations. This could have different consequences: on the one hand, the wall could undergo thermal deformation according to its constitutive behaviour, on the other hand, its thermal deformation could be partially prevented by the surrounding soil and possible over structure thus inducing additional stresses. As the primary structural role of the retaining structure must always be ensured, 2D plane strain thermo-mechanical analyses were conducted to investigate the thermal-induced mechanical effects on the diaphragm wall caused by its thermal activation. The Finite Difference Method (FDM) software FLAC [31] was used for this purpose.

3.1. Mathematical formulation

The thermal option of FLAC incorporates both conduction and advection models, but only conduction was considered in the following analyses. The heat transfer and the consequent temperature changes are coupled to the mechanical calculations at any time during a transient simulation. The coupling occurs in one direction only, i.e., the temperature may result in stress changes, but mechanical changes in the body resulting from force application do not result in temperature change. This restriction is not believed to be of great significance here, since the energy changes for quasi-static mechanical problems are usually negligible. Both soil and concrete are assumed to behave thermo-elastically and consequently their thermal deformation ε_{ij}^{T} is computed as:

$$\frac{\partial \varepsilon_{ij}^{T}}{\partial t} = \beta \frac{\partial T}{\partial t} \delta_{ij} \qquad (2)$$

where t is the time, T is the temperature, β is the coefficient of linear thermal expansion [1/°C] and δ_{ij} is the Kronecker delta. From this, constitutive equations are reformulated to solve thermal stress problems [31]. The differential equation of motion and the rate of strain-velocity relations used in the FDM are based upon mechanical considerations and are unchanged for thermo-mechanics.

3.2. Structural behaviour

Numerical analyses were performed with reference to the geometry of the reference diaphragm wall and positioning of the geothermal pipes adopted for thermo-hydraulic analyses. The mesh characteristics and

dimensions (14880 quadrilateral elements) are shown in Figure 8 together with the boundary conditions adopted. Plane strain conditions are assumed to hold true. Particular care was adopted to include the correct size of the pipes in the mesh as shown in the same Figure 8. Thermal parameters adopted are the ones given in Table 1, while mechanical parameters were chosen based on previous studies [32] and are listed in Table 6. Elastic perfectly plastic behaviour was assumed for the soil while a linear elastic behaviour for concrete.

The numerical analysis is performed in different stages. A first group of stages is used to assess the stress state in the ground resulting from the construction of the diaphragm wall and the base slab, before the geothermal system is activated. Only mechanical loading is applied during these stages. The construction of the diaphragm wall is simulated by applying appropriate mechanical parameters to the finite elements in the corresponding wall area. The excavation is then performed in three subsequent stages (two first layers of 3.2 m and a third layer of 3.1 m), obtaining a final excavation depth of 9.5 m. The base slab is afterwards installed by applying the mechanical properties of concrete to the corresponding finite elements. For the sake of simplicity, the seepage problem arising by excavating below the ground water table is not considered in the computation (TM simulations).

A second group of stages simulates the operation of the geothermal system. For these stages, the thermo-mechanical coupling is activated. Thermal boundary conditions in the model are consistent to those adopted for the thermo-hydraulic analysis previously described. The internal boundary on the car park side is assumed with a fixed temperature of 14°C, considered as the mean value year-round. The model is firstly subjected to the variation of the external air temperature only, for the period of 3 years (starting from 1st January). The external air temperature is the same as that adopted for thermo-hydraulic analyses and shown in Figure 5b. Then, the operation of the geothermal system is simulated for a period of 1000 additional days (i.e. 2 years and 270 days). This is done by applying an input temperature to the nodes of the elements which reproduce the pipes contour. The input temperature is varied along the year, following the heating and cooling cycles, by applying the corresponding values determined from the thermo-hydraulic analyses, averaged over the pipes length.

Figure 9, shows the temperature distribution in the wall and ground with colour scale labels, for two moments, representative of the summer (August) and winter (February). This is shown to be in fair agreement with the data from thermo-hydraulic analyses of Figure 7. However, some time shift is present, due to the different assumption for thermal flow and for the boundary condition adopted at the wall internal side between the thermo-hydraulic and the thermo-mechanical analyses. Also, advection is not considered in the TM analyses. While it plays a major role when assessing the temperature distribution in the ground (it was included in fact in the TH analyses), it does not influence much the temperature distribution within the wall itself. The comparison between the computed temperatures (Figs. 7 and 9) is considered in sufficient agreement to justify neglecting advection.

To evaluate the thermal induced stress strain behaviour of the wall, Figure 10 shows the horizontal displacement at the top of the diaphragm wall and the temperature variations, computed for some selected measuring points located at different depths from the top of the diaphragm wall (at 3.5 m, 9.5 m and 16 m). Selected measuring points located at the same depth (9.5 m) but at different distances from the diaphragm wall (on the pipes axis, 1.2 m and 3.2 m on the ground side) are shown instead in Figure 11. Both figures show data pertaining to the stages when the geothermal system is in operation; starting values in the plots correspond to the results of the construction stages.

It is shown that during the first three years, the temperature change is strictly dependent from the external air temperature for point A, while points B, C, D and E are ranging around a constant value due to their depth. Moreover, some deviation with time occurs to the horizontal displacement at the top of the diaphragm wall. Two full year cycles are needed before the seasonal fluctuation reaches equilibrium (this was verified by running a separate thermo-mechanical analysis where only the external air temperature effect is considered up to four years cycle).

When the geothermal system is activated, the temperature change in the points is strictly dependent from the input temperature in the pipes. This influence is reduced for point C, in the ground below the diaphragm wall. Again, an initial deviation with time of the stresses and displacements computed is experienced and

becomes negligible only after the first two years of activation. Temperature changes of points B, D and E are shown to slowly decrease while moving further from the pipes, also, the temperature peaks are shifted in time due to the thermal inertia of the soil.

Thermal cycles in the pipes cause deformation of the original wall deflection. Figures 12a and 12c show the horizontal displacements computed along the diaphragm wall vertical axis. Maximum displacement variation with respect to undisturbed state is shown for that pertaining to summer operation mode (August, Fig. 12a) and to winter operation mode (February, Fig. 12c). Also shown in the same figures are the displacements computed during mechanical loading. As the top wall deformation is not restricted, the deflection due to thermal cycles is quite evident, ranging between 16 to 22 mm (the maximum values are obtained during summer). This corresponds to a 16% displacement increase during summer and a 4% decrease during winter induced by the thermal activation of the geothermal system. The variation in terms of bending moment during heating and cooling cycles, is shown in Figures 12b and 12d. At the base of the wall, the presence of the base slab and the ground creates constraints to wall movements. Thermal induced horizontal displacements are negligible, while the corresponding stress change rises up producing a maximum bending moment of 460 kNm/m during winter (i.e. an increase of 17%). Bending moment is minimum during Summer, when the displacement is maximum, and reaches highest values in winter. The stress variations computed in the analyses are largely below the strength limits of the structure.

Similar analyses conducted by [6] have shown minor displacements at the head as an effect of thermal activation (less than 10 mm). However, in the mentioned study, despite minor variation in parameters and geometry, a major difference lied in the fact that the diaphragm wall was subjected to different constraints. A top slab was present in [6] study, whereas here the diaphragm wall is considered unrestrained at the top, to investigate a different restraint configuration. An additional numerical analysis was carried out by constraining the top of the diaphragm wall by a roller (i.e. similar conditions to the [6] study). The results confirmed lower displacements and bending moments along the diaphragm wall with respect to the non-constrained configuration. The latest, presented in this paper, can therefore be considered a conservative condition. Moreover, this is a clear (and rather obvious) indication that the mechanical effects of thermal loading on diaphragm wall are strictly function of the structural conditions. This implies that the proper construction sequence and structural behaviour need to be properly simulated in the numerical analysis to allow for reliable results to be obtained.

4. Conclusions

Based on the results of the computations described, one can draw the following conclusions:

- The horizontal configuration of pipes geometry allows maximising the heat exchange.
- The energy wall system for the conditions considered in this paper would allow to exchange between 20 to 25 W per square meter of wall, in Winter and in Summer respectively, when the ground water is static, that rises up to 40 to 50 W/m^2 when a favourable underground water flow exist.
- These figures would allow to cover energy needs of a typical apartment building, imaging to thermally activate an underground car park serving the building.
- The influence on the surrounding ground in terms of temperature variation of the groundwater flow is within 7°C at 5 m distance from the wall boundary with full recovery after the year-round cycle starting from the second year of operation.
- Bending moment and horizontal displacement at the top of the diaphragm wall increase up to 16% due to thermal activation. However, stress variations computed are largely compatible with strength limits.

The above findings are in line with research results and case study data previously published and underline the interest to improve the understanding of the geothermal process to enhance the potential use of underground infrastructures as effective and innovative heat exchangers for the future.

5. Acknowledgements

The work was performed within the framework of the Feasibility study ENERWALL (Project coordinator: Marco Barla), partially funded by the Regione Piemonte (Polo di Innovazione Regionale Enermhy) with the collaboration of Teknema Progetti srl, Torino and Resolving srl, Torino.

References

[1] L. Laloui, A. Di Donna, Energy geostructures: innovation in underground engineering, ISTE Ltd and John Wiley & Sons Inc., 2013.

[2] M. Barla, A. Di Donna, Editorial Themed issue on energy geostructures, Environ. Geotech. 3 (2016) 188–189.

[3] M. Barla, A. Di Donna, A. Perino, Application of energy tunnels to an urban environment, Geothermics. 61 (2016) 104–113.

[4] A. Di Donna, F. Cecinato, F. Loveridge, M. Barla, Energy performance of diaphragm walls used as heat exchangers, Proc. Inst. Civ. Eng. - Geotech. Eng. (2016) 1–14. doi:10.1680/jgeen.

[5] A.F. Rotta Loria, A. Di Donna, L. Laloui, Numerical Study on the Suitability of Centrifuge Testing for Capturing the Thermal-Induced Mechanical Behavior of Energy Piles, J. Geotech. Geoenvironmental Eng. 141 (2015). doi:10.1061/(ASCE)GT.1943-5606.0001318.

[6] P.J. Bourne-webb, T.M.B. Freitas, R.A.C. Gonc, Thermal and mechanical aspects of the response of embedded retaining walls used as shallow geothermal heat exchangers, 125 (2016) 130–141. doi:10.1016/j.enbuild.2016.04.075.

[7] M.E. Suryatriyastuti, H. Mroueh, S. Burlon, Understanding the temperature-induced mechanical behaviour of energy pile foundations, Renew. Sustain. Energy Rev. 16 (2012) 3344–3354. doi:10.1016/j.rser.2012.02.062.

[8] A. Di Donna, M. Barla, T. Amis, Energy geostructures: a collection of data from real applications, 15th IACMAG, Wuhan, China. (2017).

[9] D. Adam, Tunnels and foundations as energy sources—Practical applications in Austria, 5th Int. Symp. Deep Found. Bored Auger Piles (BAP V). (2009) 337–342.

[10] K. Soga, P.J. Bourne-Webb, T. Amis, C. Davidson, P. Payne, B. Amatya, Energy pile test at Lambeth College, London: geotechnical and thermodynamic aspects of pile response to heat cycles, Géotechnique. 59 (2009) 237–248. doi:10.1680/geot.2009.59.3.237.

[11] H. Brandl, Energy foundations and other thermo-active ground structures, Géotechnique. 56 (2006) 81–122. doi:10.1680/geot.2006.56.2.81.

[12] P. Riederer, G. Evers, D. Gourmez, F. Jaudin, P. Monnot, V. Pertenay, S. Pincemin, E. Wurtz, COnception de FOndations GEothermiques, (2007) 170.

[13] D. Pahud, A case study: the Dock Midfield of zurich Airport, in: L. Laloui, A. Di Donna (Eds.), Energy Geostructures Innov. Undergr. Eng., ISTE Ltd and John Wiley & Sons Inc, 2013: pp. 281–295.

[14] SIA DO 190, Utilisation de la chaleur du sol par des ouvrages de fondation et de soutènement en béton. Guide pour la conception, la realization et la maintenance, Société Suisse des ingénieurs et des architects, Switzerland, 2005.

[15] R. Markiewicz, D. Adam, Energy from earth-coupled structures, foundations, tunnels and sewers, Géotechnique. 59 (2009) 229–236.

[16] P.J. Bourne-Webb, R.A. da Costa Goncalves, T.M. Bodas Freitas, Retaining walls as heat exchangers: a numerical study, in: Proc. XVI ECSMGE Geotech. Eng. Infrastruct. Dev., (doi: 10.1680/ecsmge.60678), 2015: pp. 2499–2504. doi:10.1680/ecsmge.60678.

[17] C. Xia, M. Sun, G. Zhang, S. Xiao, Y. Zou, Experimental study on geothermal heat exchangers buried in diaphragm walls, Energy Build. 52 (2012) 50–55. doi:10.1016/j.enbuild.2012.03.054.

[18] M. Sun, C. Xia, G. Zhang, Heat transfer model and design method for geothermal heat exchange tubes in diaphragm walls, Energy Build. 61 (2013) 250–259. doi:10.1016/j.enbuild.2013.02.017.

[19] D. Sterpi, A. Angelotti, D. Corti, M. Ramus, Numerical analysis of heat transfer in thermo-active diaphragm walls, Numer. Methods Geotech. Eng. (2014) 1043–1048.

[20] T. Amis, C. Robinson, S. Wong, Integrating Geothermal Loops into the Diaphragm Walls of the Knightsbridge Palace Hotel Project, geotechnical challenges in urban regeneration, Proceeding 11th DFI / EFFC Int. Conf. London. (2010) 10.

[21] H. Brandl, Energy piles and diaphragm walls for heat transfer from and into ground, in: 3rd Int. Symp. Deep Found. Bored Auger Piles (BAP III), 1998: pp. 37–60.

[22] K. Soga, Y. Qi, H., Rui, D. Nicholson, Some considerations for designing GSHP coupled geotechnical structures based on a case study, in: 7th Int. Congr. OnEnvironmental Geotech., Melbourne, Australia, 2014.

[23] H.J.G. Diersch, DHI Wasy Software - Feflow 6.1 - Finite Element Subsurface Flow & Transport Simulation System: Reference Manual, (2009).

[24] M. Barla, A. Di Donna, Energy tunnels: concept and design aspects, Undergr. Sp. (2018). doi:https://doi.org/10.1016/j.undsp.2018.03.003.

[25] G. Barla, F. Antolini, M. Barla, M. Bonini, D. Debernardi, M. Gilardi, A. Perino, Analisi e Verifica delle Condizioni di Esercizio in Sicurezza del Palazzo Uffici Provinciali di Corso Inghilterra 7 tenuto conto del Centro Direzionale di Intesa Sanpaolo - Relazione sulle Prove di Emungimento e di Immissione - Incarico di Consulenza affi, Torino, Italy, 2013.

[26] Arpa Piemonte, No Title, Rete Di Monit. Meteoidrografica - Arpa Piemonte. (2018). http://webgis.arpa.piemonte.it/geoportalserver_arpa/.

[27] A. Di Donna, Energy walls for an underground car park, in: 25th Eur. Young Geotech. Eng. Conf., 21-24 June 2016, Sibiu, Romania, 2016.

[28] F. Cecinato, F.A. Loveridge, Influences on the thermal efficiency of energy piles, Energy. 82 (2015) 1021–1033. doi:https://doi.org/10.1016/j.energy.2015.02.001.

[29] A. Di Donna, M. Barla, The role of ground conditions and properties on the efficiency of energy tunnels, Environ. Geotech. 3 (2016).

[30] V. Corrado, I. Ballarini, S.P. Corgnati, Typology Approach for Building Stock National scientific report on the TABULA activities in Italy Ilaria Ballarini, 2012.

[31] Itasca, FLAC (Fast Lagrangian Analysisi of Continua), (2011).

[32] M. Barla, G. Barla, Torino subsoil characterisation by combining site investigations and numerical modelling, Geomech. Tunn. 5 (2012) 214–231.

Table 1 – Material properties (Barla et al., 2013).

Property	Heat carrier fluid	Ground	Concrete
Horizontal hydraulic conductivity, $k_x=k_z$ [m/s]	-	$4.15\ 10^{-3}$	10^{-16}
Vertical hydraulic conductivity, k_y [m/s]	-	$2.075\ 10^{-4}$	10^{-16}
Specific storage coefficient, S [m^{-1}]	-	10^{-4}	10^{-4}
Porosity, n [-]	-	0.25 ÷ 0.3	0.0
Heat capacity, ρc [$MJ/m^3/K$]	4.2	2.55	2.19
Thermal conductivity, λ [W/m/K]	0.65	2.26 ÷ 2.8	2.3
Longitudinal dispersivity, α_L [m]	-	3.1	-
Transverse dispersivity, α_T [m]	-	0.3	-

Table 2 – Extracted heat in the different configurations considered (fluid velocity = 0.6 m/s).

	Q ***[W]***	***Q_l*** ***[W/m]***	***Q_s*** ***[W/m^2]***
(a) VP	290.11	5.22	7.49
(b) HP - i=0.5m	324.09	4.76	8.36
(c) HP - i=1.0m	313.71	6.26	8.10

Table 3 – Extracted and injected heat with no ground water flow.

	Peak	End of cycle	Peak	End of cycle
	W/m	**W/m**	**W/m^2**	**W/m^2**
Winter	51.0	17.2	20.4	6.9
Summer	63.0	24.0	25.2	9.6

Table 4 – Extracted and injected heat with a ground water flow velocity of 1.5 m/day.

	Peak	Steady state	Peak	Steady state
	W/m	**W/m**	**W/m^2**	**W/m^2**
Winter	98.8	70.4	39.5	28.1
Summer	123.5	90.4	49.4	36.2

Table 5 – Examples of possible applications for a common building typology: apartment block (data on energy demand from Corrado et al., 2012*).*

Construction period	Total Energy need [MWh]	Exchanged heat per wall panel [kW]		Operation duration [h]	Exchanged heat per wall panel [kWh]		Number of needed panels	
		gwf=0 m/d	gwf=1.5 m/d		gwf=0 m/d	gwf=1.5 m/d	gwf=0 m/d	gwf=1.5 m/d
Today	113.5	0.27	1.1	1800.0	486.0	1962.0	233	58
1900	270.5						557	138

Table 6 – Geotechnical parameters adopted for the thermo-mechanical numerical analysis.

Property	Ground	Concrete
Unit weight [kN/m^3]	19.5	25
Elastic modulus [MPa]	215	33300
Poisson's ratio [-]	0.3	0.2
Bulk modulus [MPa]	179	18500
Shear modulus [MPa]	83	13875
Cohesion [kPa]	15	-
Friction angle [°]	38	-
Thermal conductivity, λ [W/m/K]	2.8	2.3
Linear thermal expansion, β [1/°C]	10^{-5}	$1.2 \cdot 10^{-5}$
Specific heat [J/kg°C]	1053	876

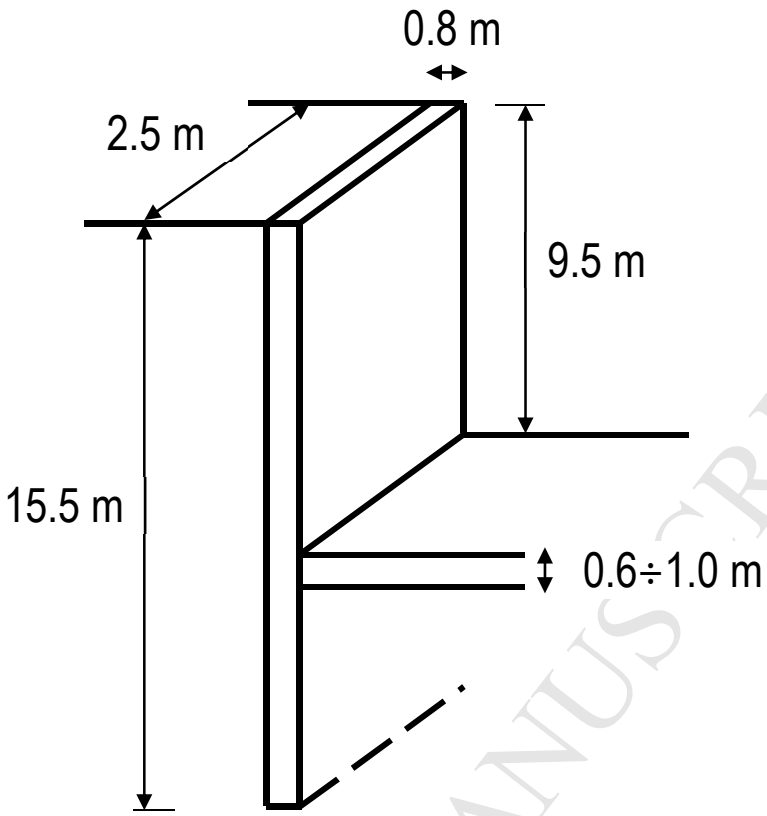

Figure 1- Geometry of the reference energy wall panel.

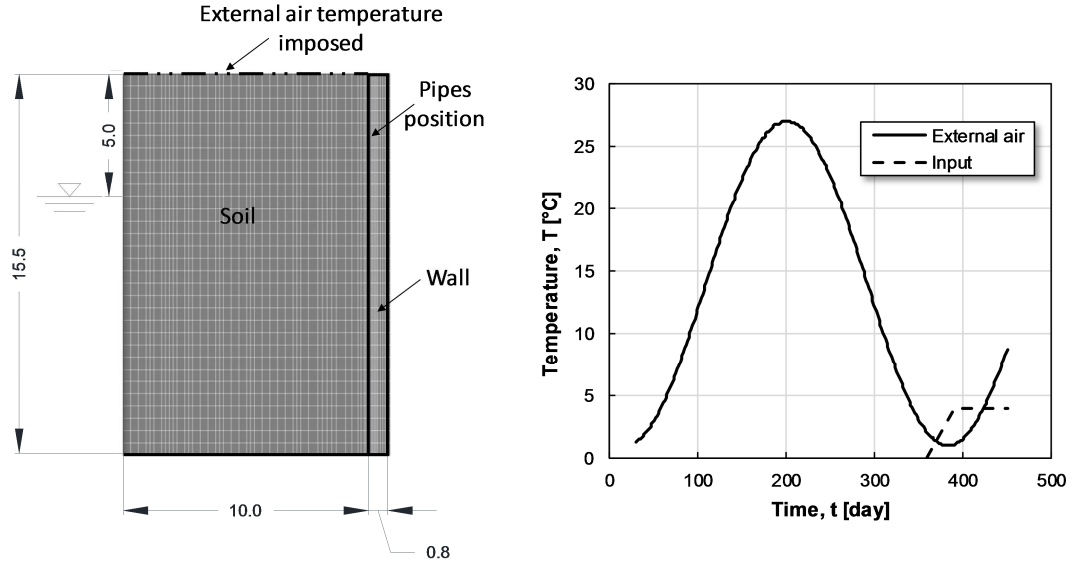

(a) (b)

Figure 2 – (a) Geometry and boundary conditions of the FE model and (b) external air and inlet temperature.

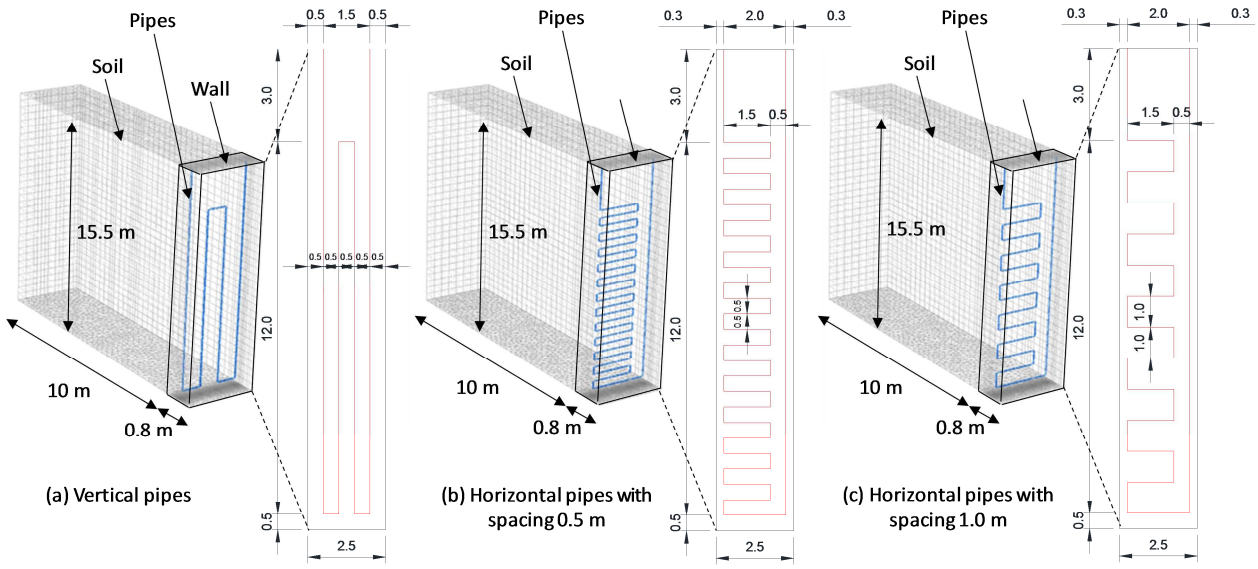

Figure 3 - Pipes configurations.

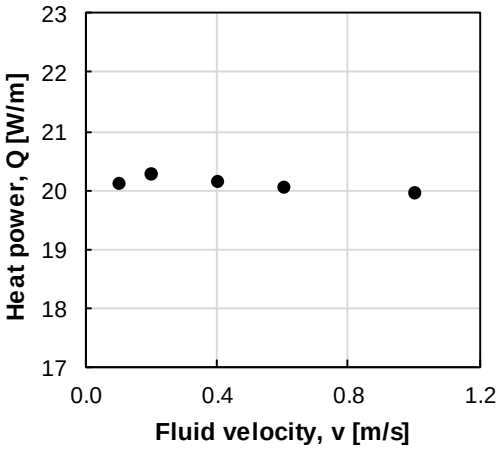

Figure 4 – Extracted heat as a function of the heat carrier fluid velocity in the pipes.

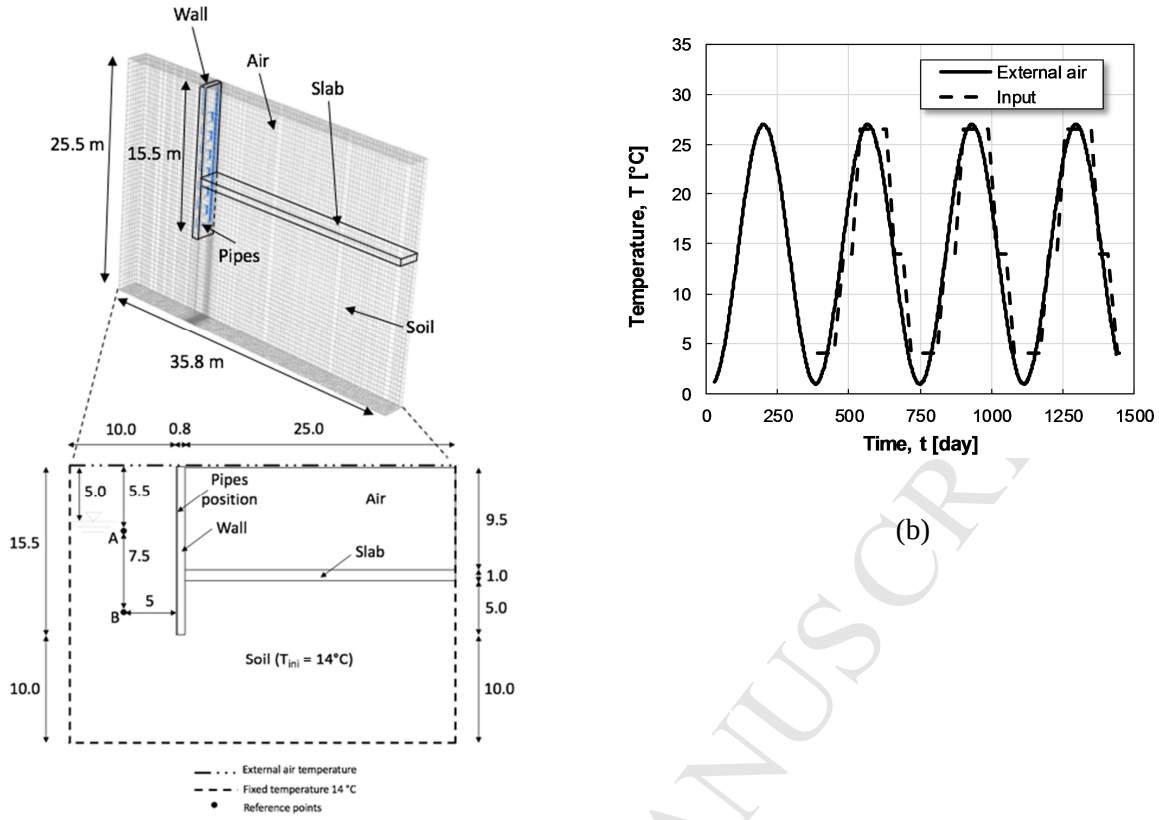

Figure 5 – (a) Geometry of the model and (b) imposed cyclic inlet temperature and external air temperature variation in Torino.

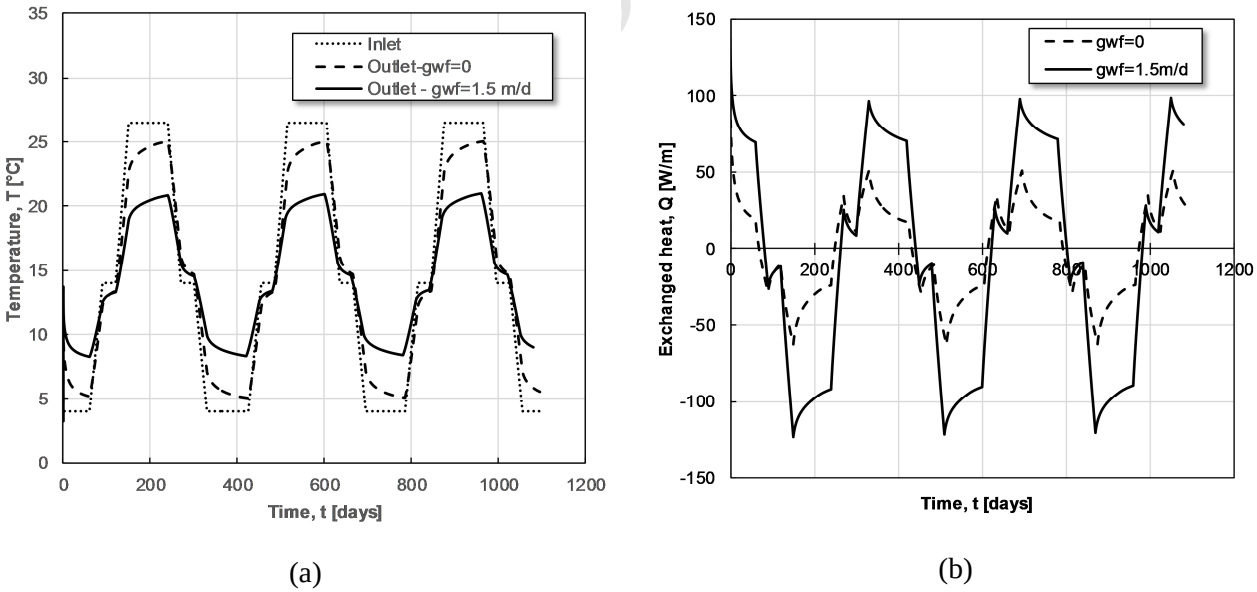

Figure 6 – (a) Inlet and outlet temperature in the pipes and (b) exchanged heat during three years' simulation, in the case of 0 and 1.5 m/day of ground water flow.

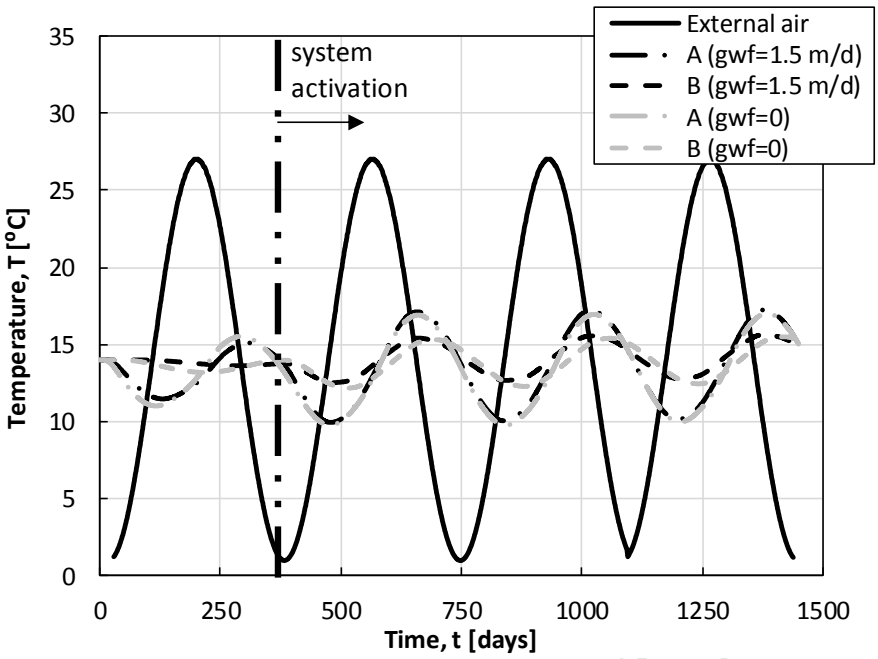

Figure 7 – Temperature variation in the ground 5 m far from the wall at different depths, in the case of 0 and 1.5 m/day of ground water velocity.

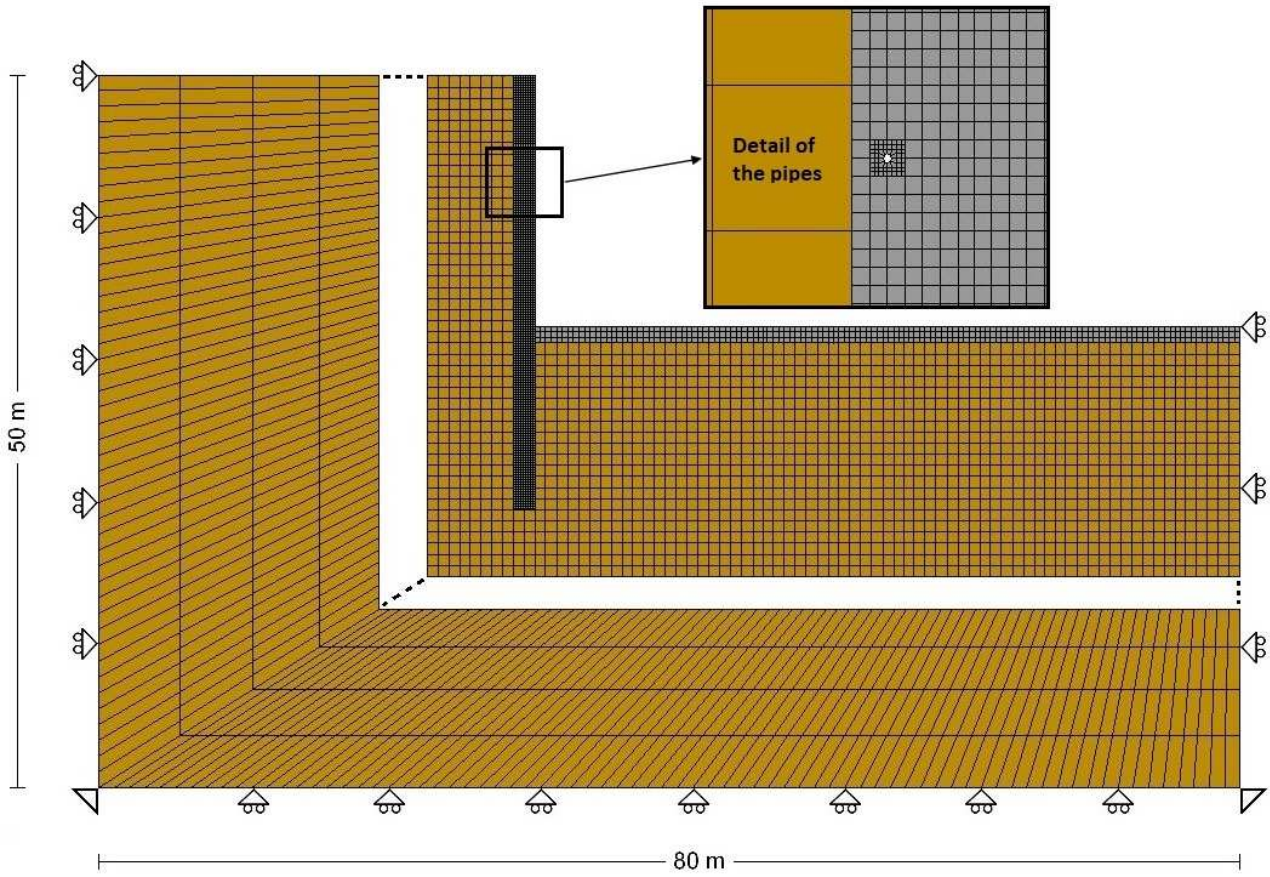

Figure 8 – Finite difference mesh adopted for thermo-mechanical analyses: model, size, boundary conditions and detail of the mesh in the pipe area.

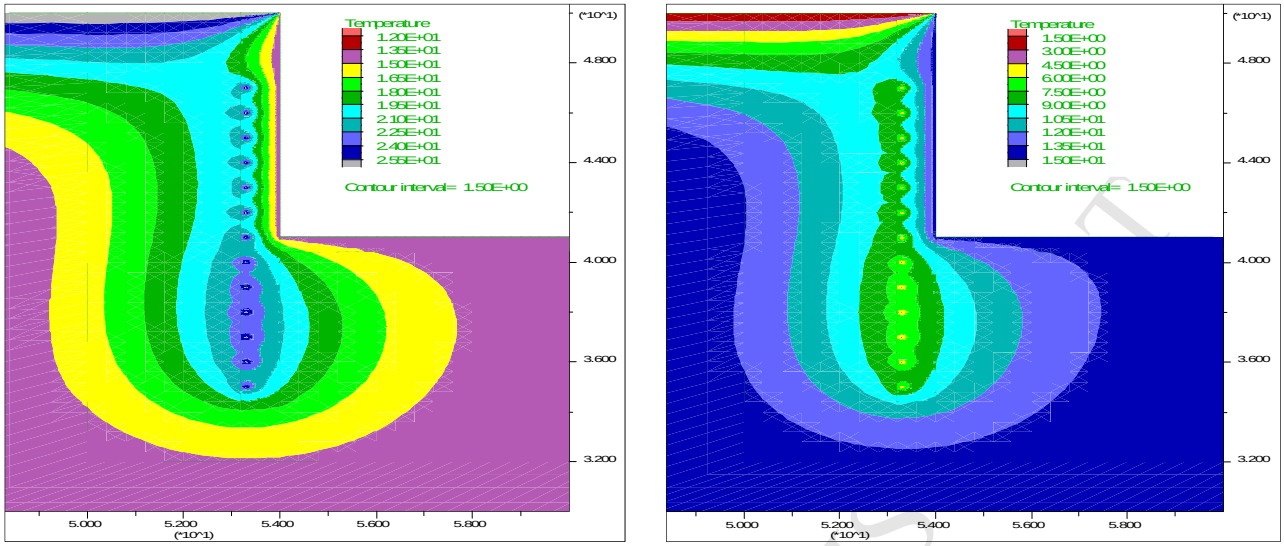

(a) (b)

Figure 9 – Temperature distribution in °C in the ground in August (a) and February (b) with the geothermal system activated.

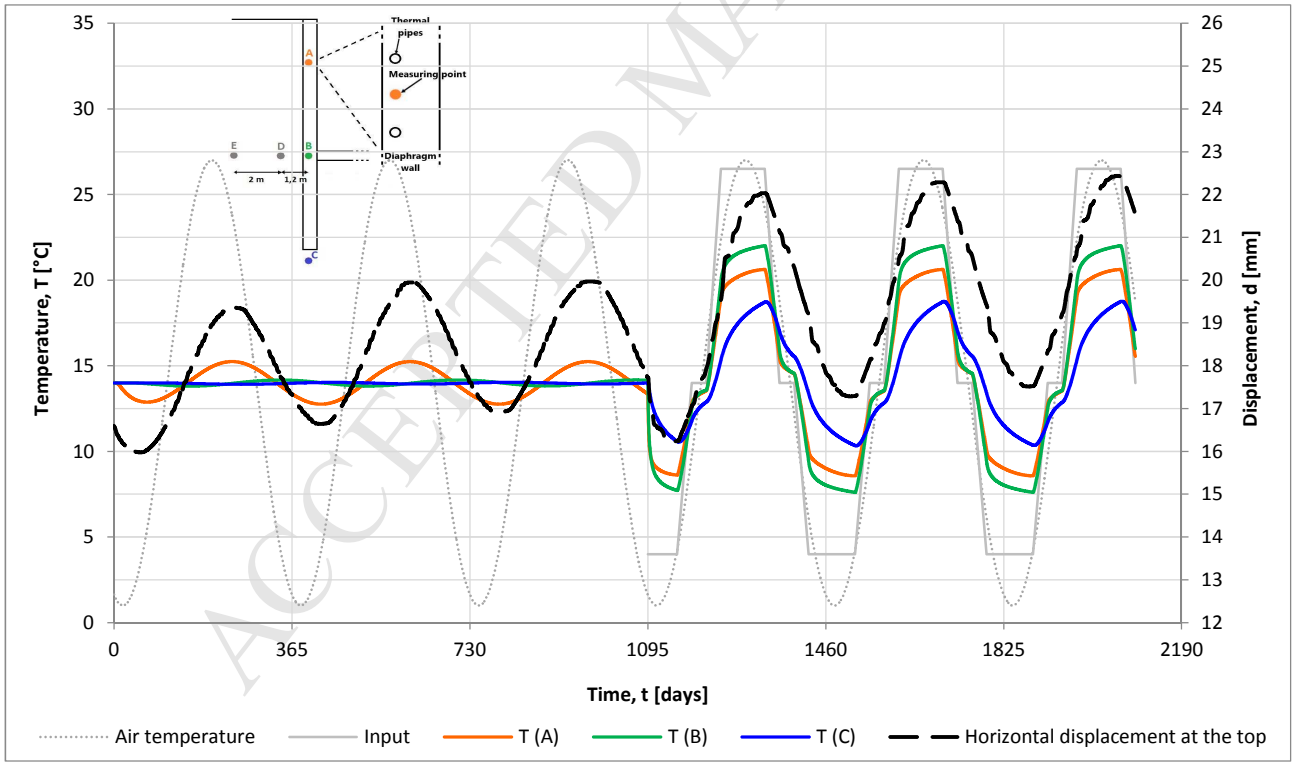

Figure 10 – Displacement at the top of the diaphragm wall, input temperature variation in the pipes and external air temperature assumed during computation compared to that computed at specific measuring points (A, B, C).

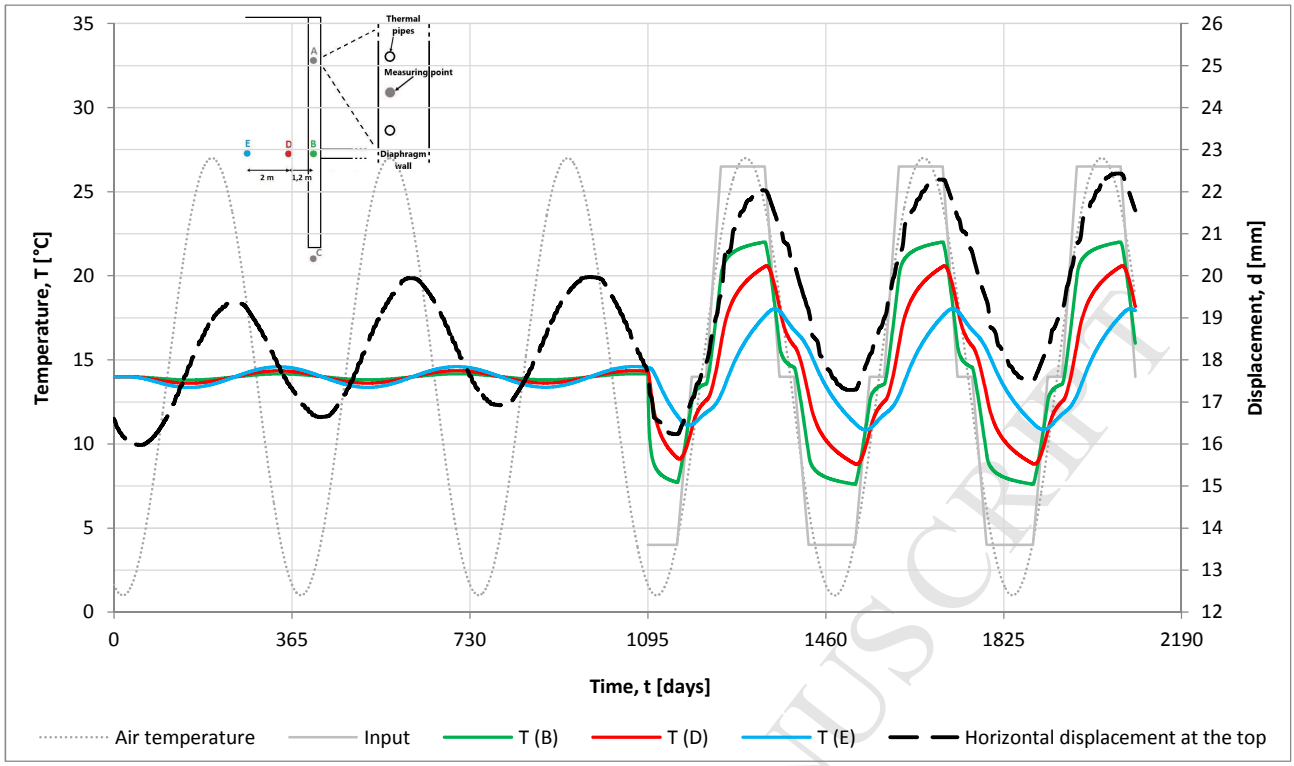

Figure 11 – Displacement at the top of the diaphragm wall, input temperature variation in the pipes and external air temperature assumed during computation compared to that computed at specific measuring points (B, D, E).

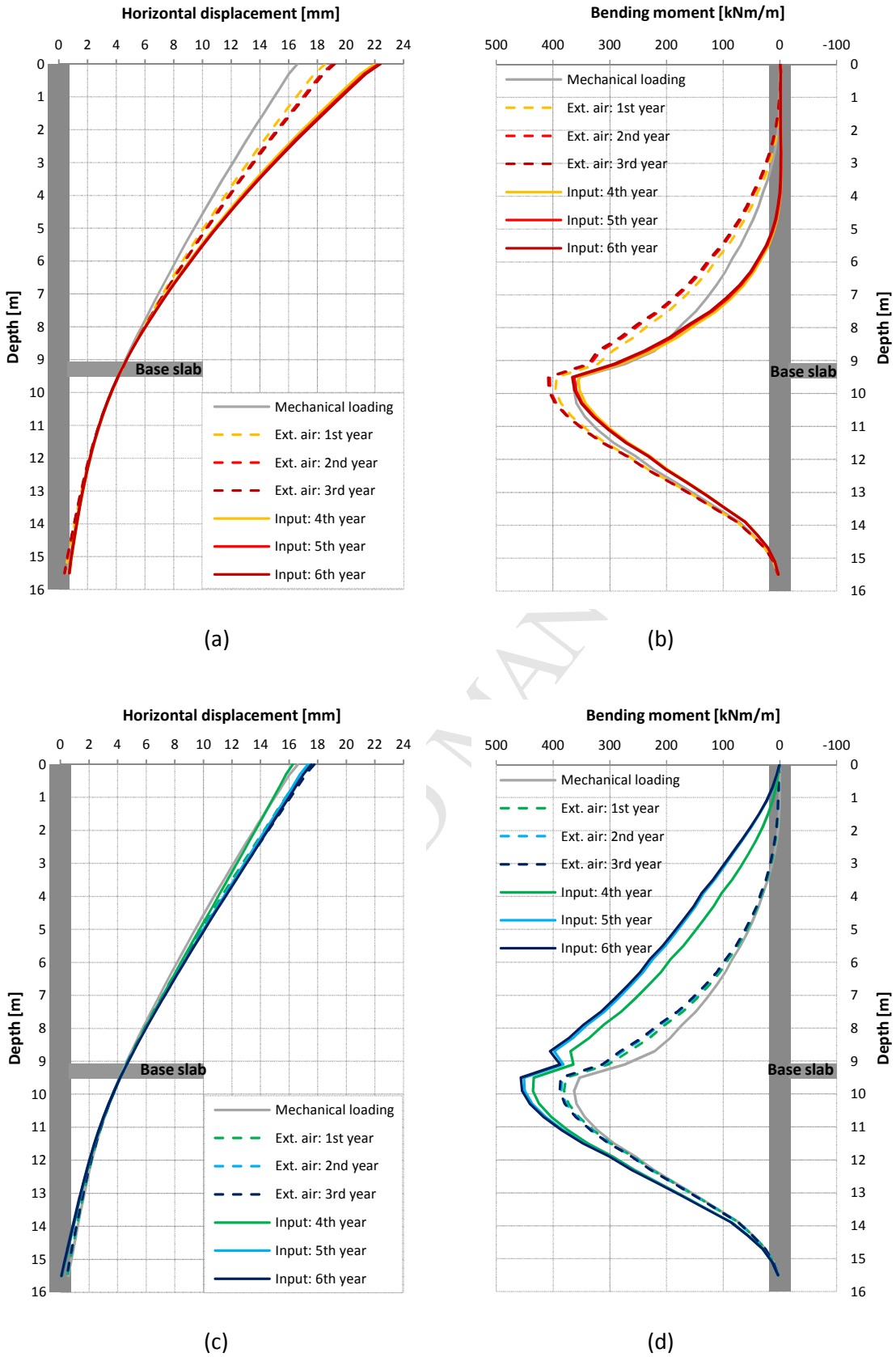

Figure 12 – Bending moment and horizontal displacement change with: mechanical loading, external air and the activation of the geothermal system in Summer (August, (a), (b)) and Winter (February, (c), (d)).

- Thermal and mechanical aspects of energy walls are discussed.
- The horizontal configuration of pipes geometry allows maximising the heat exchange.
- Heat exchange between 20 to 25 W/m^2 with static ground water.
- Heat exchange between 40 to 50 W/m^2 with favourable groundwater flow.
- Bending moment increase up to 16% due to thermal activation.